Supporting Information

Quadruple Bonding in the Ground and Low-Lying Excited States of the Diatomic Molecules TcN, RuC, RhB, and PdBe

Demeter Tzeli*[a,b] and Ioannis Karapetsas [a]

[a] Laboratory of Physical Chemistry, Department of Chemistry, National and Kapodistrian University of Athens, Panepistimiopolis Zografou, Athens 157 84, Greece

[b] Theoretical and Physical Chemistry Institute, National Hellenic Research Foundation, 48 Vassileos Constantinou Ave., Athens 116 35, Greece

E-mail: tzeli@chem.uoa.gr, dtzeli@eie.gr

Tel: +30-210-727-4307, +30-210-727-3811

Fax: +30-210-727-3794

Table S1. Energy Separation (eV) of atomic states of M, M = Tc, Ru, Rh, and Pd metals at MRCISD, MRCISD+Q, and RCCSD(T)/aug-cc-pV5Z-PP$_M$.

	Rh		**Ru**	
Method[a]	***a*** ^{2}**D** ← ***a*** ^{4}**F**	***a*** ^{2}**F** ← ***a*** ^{4}**F**	***a*** ^{3}**F** ← ***a*** ^{5}**F**	***b*** ^{3}**F** ← ***a*** ^{5}**F**
	$4d^9 \leftarrow 4d^8(^3F)5s^1$	$4d^8(^3F)5s^{1\downarrow} \leftarrow 4d^8(^3F)5s^{1\uparrow}$	$4d^7(a^4F)5s^{1\downarrow} \leftarrow 4d^7(a^4F)5s^{1\uparrow}$	$4d^8 \leftarrow 4d^7(a^4F)5s^1$
MRCI	0.476	0.632	0.858	1.301
MRCI+Q	0.386	0.593	0.794	1.223
RCCSD(T)	0.368	0.774		1.147
Expt.[b,c]	0.410	0.706	0.811	1.131
Expt.[b,d]	0.342	0.632	0.782	1.092
	Tc			
	^{6}**D** ← ^{6}**S**	^{4}**D** ← ^{6}**S**	^{4}**P** ← ^{6}**S**	^{4}**F** ← ^{6}**S**
	$4d^6(^6D)5s^{1\uparrow} \leftarrow 4d^55s^2$	$4d^6(^6D)5s^{1\downarrow} \leftarrow 4d^55s^2$	$4d^6(^3P)5s^1 \leftarrow 4d^55s^2$	$4d^7 \leftarrow 4d^55s^2$
MRCI	0.378	1.422	2.000	2.476
MRCI+Q	0.556	1.543	2.101	2.505
RCCSD(T)	0.567			
Expt.[b,c]	0.319	1.304	1.643	1.827
Expt.[b,d]	0.406	1.368	1.711	2.332
	Pd		**N**	**Be**
	^{3}**D** ← ^{1}**S**	^{1}**D** ← ^{1}**S**	^{2}**D** ← ^{4}**S**	^{3}**P** ← ^{1}**S**
	$4d^95s^{1\uparrow} \leftarrow 4d^{10}$	$4d^95s^{1\downarrow} \leftarrow 4d^{10}$	$2s^22p^3 \leftarrow 2s^22p^3$	$2s^12p^1 \leftarrow 2s^2$
MRCI	0.949	1.349	2.415	2.736
MRCI+Q	1.005	1.378	2.383	2.736
RCCSD(T)	1.068		2.651	2.732
Expt.[b,c]	0.814	1.251	2.384	2.725
Expt.[b,d]	0.875	1.378	2.384	2.725

[a] Q refer to the Davidson correction.
[b] Reference 53.
[c] Energy separation between the term having the lowest in energy spin-orbit coupling angular momentum quantum number J.
[d] Average term.

Table S2. Energy Separation (eV) of atomic states of M, M = Tc, Ru, Rh, and Pd metals involved in the minimum of the $^1\Sigma^+$ and $^3\Delta$ states of the diatomic MX, X=Be-N at MRCISD, MRCISD+Q, and RCCSD(T)/aug-cc-pV5Z-PP$_M$.

	Tc	**Ru**	**Rh**	**Pd**
Method[a]	**^{4}F ← ^{6}D**	***b*** **^{3}F ← *a* ^{5}F**	***a*** **^{2}D ← *a*^{4}F**	**^{3}D ← *a*^{1}S**
	$4d^7 \leftarrow 4d^6 5s^1$	$4d^8 \leftarrow 4d^7(a^4F)5s^1$	$4d^9 \leftarrow 4d^8(^3F)5s^1$	$4d^9 5s^1 \leftarrow 4d^{10}$
MRCI	2.098	1.301	0.476	0.949
MRCI+Q	1.949	1.223	0.386	1.005
RCCSD(T)		1.147	0.368	1.068
Expt.[b,c]	1.508	1.131	0.410	0.814
Expt.[b,d]	1.926	1.092	0.342	0.875

[a] Q refer to the Davidson correction.
[b] Reference 53.
[c] Energy separation between the term having the lowest in energy spin-orbit coupling angular momentum quantum number J.
[d] Average term.

Table S3. Energy Separation (eV) of atomic states of M, M = Tc, Ru, Rh, and Pd metals involved in the $^3\Delta$ and $^1\Delta$ states of the diatomic MX, X=Be-N at MRCISD, MRCISD+Q, and RCCSD(T)/aug-cc-pV5Z-PP$_M$.

	Tc	**Ru**	**Rh**	**Pd**
Method[a]	**^{4}D ← ^{6}D**	***a*** **^{3}F ← *a* ^{5}F**	***a*** **^{2}F ← *a* ^{4}F**	**^{3}D**$(4d^9 5s^1)$
	$4d^6 5s^{1\downarrow} \leftarrow 4d^6 5s^{1\uparrow}$	$4d^7(a^4F)5s^{1\downarrow} \leftarrow 4d^7(a^4F)5s^{1\uparrow}$	$4d^8(^3F)5s^{1\downarrow} \leftarrow 4d^8(^3F)5s^{1\uparrow}$	Same state
MRCI	1.044	0.858	0.632	0
MRCI+Q	0.987	0.794	0.593	0
RCCSD(T)			0.774	0
Expt.[b,c]	0.985	0.811	0.706	0
Expt.[b,d]	0.962	0.782	0.632	0

[a] Q refer to the Davidson correction.
[b] Reference 53.
[c] Energy separation between the term having the lowest in energy spin-orbit coupling angular momentum quantum number J.
[d] Average term.

Table S4. Absolute Energies E (hartree), Bond Lengths r_e (Å), Binding Energies D_e (kcal/mol), Harmonic Frequencies and Anharmonic Corrections ω_e, $\omega_e x_e$ (cm^{-1}), Rotational Vibrational Couplings α_e (cm^{-1}), Centrifugal Distortions $\overline{D}_e$(cm^{-1}), Total Mulliken Charges on Metal q_M, Dipole Moments μ (Debye) and Energy Differences T_e (kcal/mol), at various levels of theory of the TcN, RuC, RhB, and PdBe molecules.

State	Methods[a]	E	r_e	D_e[a](D_e[d])[b]	D_e^{gs} [b]	ω_e	$\omega_e x_e$	$\alpha_e(10^{-3})$	$\overline{D}_e$ (10^{-6})	q_M	<μ>	μ_{FF}[c]	T_e
					TcN								
$X^3\Delta$	MRCISD	-134.671268	1.5966	120.9	109.6	1109.4	5.24	3.12	0.513	-0.50	1.743	2.260	0.00
	MRCISD+Q	-134.697263	1.5992	123.3	111.6	1101.0	5.23	3.16	0.516			2.389	0.00
	RCCSD(T)	-134.703334	1.5946	123.3	110.2	1132.0	4.77	2.94	0.497			2.391	0.00
	MS-CASPT2 [d]		1.605		121.5	1085					2.38		0.0
$a^1\Sigma^+$	MRCISD	-134.645677	1.5897	149.0(160.0)	93.6	1134.9	4.45	2.82	0.503	-0.46	4.615	4.543	16.05
	MRCISD+Q	-134.674219	1.5930	150.8(160.1)	97.1	1124.2	4.46	2.86	0.507			4.512	14.45
	RCCSD(T)	-134.677936	1.5890	144(153)	94.3	1144.3	4.25	2.73	0.497			4.483	15.93
$b^1\Delta$	MRCISD	-134.645711	1.5858	129.9	93.5	1146.3	4.84	2.96	0.501	-0.54	1.066	1.407	16.03
	MRCISD+Q	-134.673091	1.5880	131.4	96.4	1137.4	4.86	3.01	0.504			1.671	15.16
	MS-CASPT2 [d]		1.591			1131					0.20		18.8
$A^3\Sigma^-(1)$	MRCISD	-134.641020	1.6300	90.6	90.6	1018.4	6.17	3.57	0.538	-0.56	0.767	1.575	18.97
	MRCISD+Q	-134.673531	1.6291	96.7	96.7	1023.2	6.09	3.53	0.534			1.371	14.88
	MS-CASPT2 [d]		1.640		105	1003					0.25		7.6
$c^5\Pi$	MRCISD	-134.632815	1.6786	97.0	85.5	938.6	4.76	3.07	0.531	-0.29	2.795	3.061	24.12
	MRCISD+Q	-134.665037	1.6733	103.1	91.4	945.1	4.68	3.12	0.534			2.970	20.21
	MS-CASPT2 [d]		1.670		103	947					2.77		18.6
$^9\Sigma^-(1)$	MRCISD	-134.500328	2.2628		2.32	461.1	3.69	2.29	0.366	+0.28	2.985	2.582	107.20
	MRCISD+Q	-134.519893	2.273		0.30	442.3	3.35	2.48	0.386			2.445	111.24
	MS-CASPT2 [d]		2.144			630					0.39		107.4
$^9\Sigma^-(2)$	MRCISD	-134.492504	2.2191	8.70	-2.59	457.2	8.67	3.78	0.419	+0.12	0.958	2.515	112.11
	MRCISD+Q	-134.530861	2.193	16.4	4.71	527.7	6.35	2.67	0.338			3.622	104.36
					RuC								
$X^1\Sigma^+$	MRCISD	-132.019410	1.6018	164.1(174.4)	141.3	1116.4	4.73	3.61	0.736	-0.73	4.205	4.156	0.00
	MRCISD+Q	-132.047646	1.6042	165.5(176.4)	145.9	1109.7	4.73	3.63	0.738			4.107	0.00

	RCCSD(T)	-132.055640	1.5989	(176.5)	150.1	1130.4	3.82	3.55	0.725			3.970	0.00
					154.0±3.0[h]								
	Expt		1.60790(9)[e,f,g]		151.0±3.0[i]	1100.0(1.5)[e]	5.3(0.3)[e]				4.09(14)[j]		
			1.605485(2)[w]		145.5±2.5[f]								
	MRCI[k]		1.614	135		1070							0
	Rel_MRCI[k]		1.616	129		1085					4.018		0
	FO+MRCI[l]		1.634			1085					4.208		0
	Expt[m]			162.5[m]		1039.14[m]	4.75[m]						
	Expt[m]					954.56[m]	5.39[m]						
***a*^{3}Δ**	MRCISD	-132.015674	1.6304	138.9	138.9	1044.7	4.91	3.79	0.756	-0.75	1.466	1.977	2.34
	MRCISD+Q	-132.044250	1.6332	143.8	143.8	1039.8	4.97	3.79	0.755			2.074	2.13
	Expt		1.63515[e,f,n,g]	146.3±2.5[p,g]		1038.77(0.39)[e,g,n]	4.64(0.13)[e,n]				1.95(2)[q]		0.217[f]
	MRCI[k]		1.632	118		1041							16.6
	Rel_MRCI[k]		1.632	127		1064					0.897		2.61
	FO+MRCI[l]		1.667			1034					1.522		-7.91(-3.78)
***A*^{1}Δ**	MRCISD	-131.993741	1.6203	148.3	125.2	1068.8	5.21	3.85	0.749	-0.81	1.122	1.410	16.11
	MRCISD+Q	-132.023778	1.6230	150.5	130.9	1063.1	5.25	3.87	0.750			1.585	14.98
	Expt		1.6343[e,n,g]			1032[e,n,o]							5.84[e]
	MRCI[k]		1.619	106		1061					0.069		29.0
	Rel_MRCI[k]		1.618	112		1086							17.3
	FO+MRCI[l]		1.649			1052					0.712		6.66(10.2)
					RhB								
***X*^{1}Σ$^+$**	MRCISD	-134.437548	1.6853	134.2	125.4	943.6	4.43	4.03	0.955	-0.77	3.357	3.254	0.0
	MRCISD+Q	-134.467191	1.6873	135.1	126.2	938.3	4.32	4.06	0.960			3.160	0.0
	RCCSD(T)	-134.479970	1.6872	135.1	126.6	942.1	3.78	3.87	0.952			2.865	0.0
	CCSD(T)[r]		1.689	130	121								
	Expt[s,t,u]		1.69[s]		112.8±5.0[t]	920[s]							
					121.1[u]								
	MS-CASPT2[v]		1.694	129		924					4.54		
***a*^{3}Δ**	MRCISD	-134.396584	1.7645	99.7	99.7	803.7	4.84	4.28	1.000	-0.72	1.189	1.807	25.7
	MRCISD+Q	-134.427386	1.7678	101.2	101.2	799.3	4.78	4.45	0.999			1.871	25.0
	MS-CASPT2 [v]		1.782	101		805					1.76		21.0
***A*^{1}Δ**	MRCISD	-134.383247	1.7608	102.3(105.9[j])	91.3	810.0	4.52	4.22	0.997	-0.79	1.635	1.326	34.1
	MRCISD+Q	-134.415471	1.7610	102.6(107.4)	93.7	818.3	5.62	4.39	0.975			1.256	32.5
	MS-CASPT2 [v]		1.777	104		793					0.86		26.6

						PdBe							
$X^1\Sigma^+$	MRCISD	-141.666226	1.9123	48.5	48.5	638.1	4.17	5.28	1.680	-0.65	1.670	1.219	0.00
	MRCISD+Q	-141.696770	1.9117	52.8	52.8	635.8	4.43	5.44	1.6953			1.007	0.00
	RCCSD(T)	-141.713544	1.9101	49.7	49.7	636.2	2.99	5.11	1.7046			0.786	0.00
$a^3\Sigma^+$	MRCISD	-141.608695	2.0314	32.6(95.5)	12.4	548.4	8.06	5.94	1.580	-0.56	1.164	1.037	36.10
	MRCISD+Q	-141.640403	2.0272	37.6(100.6)	17.4	620.2	17.0	6.43	1.182			0.861	35.37
$b^3\Delta$	MRCISD	-141.588994	2.1533	20.2(83.1)	0.03	463.7	4.20	4.83	1.560	-0.51	1.658	1.244	48.46
	MRCISD+Q	-141.619011	2.1466	24.2(87.2)	3.97	462.6	4.56	5.13	1.598			0.998	48.79
$A^1\Delta$	MRCISD	-141.582777	2.1382	25.4(79.2)	-3.87	490.3	2.63	3.87	1.456	-0.51	2.035	1.575	52.37
	MRCISD+Q	-141.613786	2.1324	29.1(83.9)	0.69	487.1	3.13	4.21	1.499			1.244	52.07

[a] Internally contracted MRCI; +Q refers to the multireference Davidson correction. [b] D_e[a]: Adiabatic dissociation energy; D_e[d]:Diabatic dissociation energy; D_e[gs]: Dissociation energy with respect to the ground state products. [c] Ground state products [c] $\mu_{FF} = \delta E / \delta E$. [d] Ref. 18; MS-CASPT2/4ζ-ANO-RCC. [e] Ref. 25. [f] Ref. 26. [g] R_0, D_0 values. [h] Ref. 21. [i] Ref. 22. [j] Ref. 30. [k] Ref. 28; MRCI/[11s9p5d2f]$_{Ru}$[4s3p1d]$_C$. [l] Ref. 29; using RECPs: (5*s*4*p*4*d*2f$_{Ru}$14*s*4*p*2*d*$_C$). In parenthesis MRCISD+Q . [m] Ref. 23; the state has not been identified as a Σ^+ or a Δ state. [n] Ref. 19-20. [o] $\Delta G_{1/2}$. [p] Ref. 24. [q] Ref. 31; 1.95(2) for [0.1] $^3\Delta_3$ and 1.86(2) Debye for [0.9] $^3\Delta_2$. [r] Ref. 9; CCSD(T)/aug-cc-pXQZ$_B$(-PP$_{Rh}$). [s] Ref. 36. [t] Ref. 35; D_0^0(gas). [u] Ref. 37; D_0 values. [v] Ref. 39; MS-CASPT2/4ζ-ANO-RCC. [w] Ref. 38; R_e.

Table S5. Mulliken (first line), NBO(second line), and CM5 (third line) MRCI population analysis and total charges on metals.

	5s	$5p_z$	$4d_{z2}$	$4d_{x2y2}$	$5p_x$	$4d_{xz}$	$5p_y$	$4d_{yz}$	$4d_{xy}$	2s	$2p_z$	$2p_x$	$2p_y$	q_M
							TcN							
$X^3\Delta$	0.98	0.23	1.17	1.97	0.06	0.94	0.06	0.94	0.99	1.53	1.01	0.94	0.94	-0.50
	0.87	0.00	0.77	1.99	0.00	0.99	0.00	0.99	0.99	1.90	1.41	0.98	0.98	+0.31
														+0.56
$a^1\Sigma^+$	0.17	0.14	1.12	1.97	0.06	0.90	0.06	0.90	0.97	1.53	0.96	0.99	0.99	-0.46
	0.89	0.02	0.97	1.95	0.00	0.93	0.00	0.93	0.95	1.91	1.23	1.06	1.06	+0.31
$b^1\Delta$	0.97	0.22	1.17	0.99	0.06	0.93	0.06	0.93	1.96	1.53	0.98	0.97	0.97	-0.54
	0.89	0.02	0.95	0.99	0.00	0.90	0.00	0.90	1.99	1.91	1.29	1.08	1.08	+0.31
$A^3\Sigma^-$	1.75	0.20	1.31	0.98	0.07	1.02	0.07	1.02	0.98	1.49	1.12	0.88	0.88	-0.56
	0.86	0.00	1.96	0.99	0.00	0.91	0.00	0.91	0.99	1.90	1.22	1.08	1.08	+0.32
$c^5\Pi$	0.97	0.22	1.18	0.99	0.05	1.10	0.18	1.44	0.99	1.57	0.99	0.81	1.28	-0.29
	0.83	0.06	1.16	0.99	0.01	1.10	0.01	1.20	0.99	1.91	1.02	0.92	1.71	+0.60
$^9\Sigma^-(1)$	1.04	0.46	1.12	0.99	0.03	0.99	0.03	0.99	0.99	1.82	1.50	0.95	0.95	+0.28
	0.99	0.13	1.10	0.99	0.01	0.99	0.01	0.99	0.99	1.97	1.77	0.99	0.99	+0.76
$^9\Sigma^-(2)$	1.01	0.30	1.49	0.99	0.01	0.99	0.01	0.99	0.99	1.84	1.28	0.98	0.98	+0.12
	0.92	0.12	1.12	1.00	0.01	0.99	0.01	0.99	1.00	1.96	1.83	0.99	0.99	+0.80
							RuC							
$X^1\Sigma^+$	0.30	0.25	1.47	1.96	0.06	1.26	0.06	1.26	1.96	1.26	0.63	0.65	0.65	-0.73
	0.93	0.01	0.56	1.95	0.00	1.25	0.00	1.25	1.95	1.85	0.70	0.73	0.73	+0.04
														+0.40
$a^3\Delta$	1.06	0.33	1.50	1.97	0.06	1.32	0.06	1.32	0.99	1.27	0.73	0.59	0.59	-0.75
	0.87	0.00	1.46	1.96	0.00	1.29	0.00	1.29	0.98	1.87	0.86	0.66	0.66	+0.09
														+0.32
$A^1\Delta$	1.10	0.33	1.54	1.97	0.06	1.31	0.06	1.31	0.99	1.24	0.69	0.60	0.60	-0.81
	0.93	0.01	1.41	1.96	0.00	1.30	0.00	1.30	0.98	1.85	0.75	0.70	0.70	+0.04
							RhB							
$X^1\Sigma^+$	0.49	0.27	1.69	1.97	0.05	1.56	0.05	1.56	1.97	1.13	0.35	0.34	0.34	-0.77
	0.11	0.00	1.71	1.99	0.00	1.58	0.00	1.58	1.99	1.81	0.38	0.38	0.38	-0.03
														+0.48
$a^3\Delta$	1.17	0.33	1.73	1.97	0.04	1.67	0.04	1.67	0.99	1.18	0.48	0.27	0.27	-0.72
	0.93	0.02	1.74	1.98	0.00	1.68	0.00	1.68	0.99	1.80	0.51	0.29	0.29	-0.08
														+0.36
$A^1\Delta$	1.27	0.25	1.77	1.97	0.04	1.67	0.04	1.67	0.99	1.03	0.53	0.28	0.28	-0.79
	0.92	0.01	8.13							1.67	1.18			-0.12
							PdBe							
$X^1\Sigma^+$	0.78	0.24	1.85	1.98	0.02	1.85	0.02	1.85	1.98	0.95	0.13	0.11	0.11	-0.65
	0.37	0.05	1.88	1.99	0.01	1.91	0.01	1.91	1.99	1.57	0.11	0.07	0.07	-0.18
														-0.04
$\alpha^3\Sigma^+$	1.06	0.16	1.50	1.98	0.02	1.88	0.02	1.88	1.98	0.74	0.49	0.08	0.08	-0.56
	1.38	0.07	1.32	1.95	0.01	1.80	0.01	1.80	1.95	1.38	0.20	0.03	0.03	-0.35
														-0.09
$b^3\Delta$	1.46	0.19	1.91	1.98	0.02	1.94	0.02	1.94	0.99	0.92	0.45	0.04	0.04	-0.51
	1.33	0.06	1.94	2.00	0.01	1.95	0.01	1.95	1.00	1.39	0.23	0.02	0.02	-0.32
$A^1\Delta$	1.48	0.18	1.91	1.98	0.02	1.93	0.02	1.93	0.99	0.86	0.50	0.04	0.04	-0.51
	1.34	0.08	1.94	2.00	0.01	1.95	0.01	1.95	1.00	1.32	0.28	0.02	0.02	-0.34

Table S6. Methodology.

	CSFs		CSFs	CSFs	CAS	MRCI		
	CAS	Coef [a]	MRCI	icMRCI	C_0	C_0	Main MRCI CSFs	RCCSD(T)
TcN								
$X^3\Delta$	5154/5196	0.960	1,075,778,714	4,884,866	0.935	0.900	$\left\|X\,^3\Delta\right\rangle_{A_1+A_2} \cong 0.90\left\|\frac{1}{\sqrt{2}}\left(1\sigma^2 2\sigma^2 3\sigma^1 1\pi_x^2 1\pi_y^2\right)\left(1\delta_+^1 1\delta_-^2 + 1\delta_+^2 1\delta_-^1\right)\right\rangle$	1,262,167
$^1\Sigma^+$	3588	0.959	587,898,192	3,356,266	0.943	0.903	$\left\|\,^1\Sigma^+\right\rangle \cong 0.90\left\|1\sigma^2 2\sigma^2 1\pi_x^2 1\pi_y^2 1\delta_+^2 1\delta_-^2\right\rangle$	1,254,468
$^1\Delta$	3588/3392	0.959	587,898,192	3,356,266	0.936	0.901	$\left\|^1\Delta\right\rangle_{A_1+A_2} \cong 0.90\left\|\frac{1}{\sqrt{2}}\left(1\sigma^2 2\sigma^2 3\bar{\sigma}^1 1\pi_x^2 1\pi_y^2\right)\left(1\delta_+^1 1\delta_-^2 + 1\delta_+^2 1\delta_-^1\right)\right\rangle$	
$^3\Sigma^-$	5196	0.967	1,075,778,714	4,884,866	0.915	0.887	$\left\|\,^3\Sigma^-\right\rangle \cong 0.89\left\|1\sigma^2 2\sigma^2 3\sigma^2 1\pi_x^2 1\pi_y^2 1\delta_+^1 1\delta_-^1\right\rangle$	
$^5\Pi$	2060/2060	0.953	660,285,090	3,122,076	0.914	0.883	$\left\|\,^5\Pi\right\rangle_{B_1+B_2} \cong 0.88\left\|\frac{1}{\sqrt{2}}\left(1\sigma^2 2\sigma^2 3\sigma^1\right)\left(1\pi_x^2 1\pi_y^2 2\pi_y^1 + 1\pi_x^2 2\pi_x^1 1\pi_y^2\right)1\delta_+^1 1\delta_-^1\right\rangle$	
$^9\Sigma^-(1)$	12	0.964	13,465,520	1,206,239	1.000	0.963	$\left\|\,^9\Sigma^-\right\rangle \cong 0.96\left\|1\sigma^2 2\sigma^2 3\sigma^1 4\sigma^1 1\pi_x^1 2\pi_x^1 1\pi_y^1 2\pi_y^1 1\delta_+^1 1\delta_-^1\right\rangle$	
$^9\Sigma^-(2)$	12	0.943	13,465,520	1,206,239	0.714	0.776	$\left\|\,^9\Sigma^-(2)\right\rangle \cong 0.78\left\|1\sigma^2 2\sigma^2 1\pi_x^1 2\pi_x^1 1\pi_y^1 2\pi_y^1 1\delta_+^1 1\delta_-^1\right\rangle$	
RuC								
$X^1\Sigma^+$	3588	0.959	587,898,192	3,356,266	0.935	0.899	$\left\|X\,^1\Sigma^+\right\rangle \cong 0.90\left\|1\sigma^2 2\sigma^2 1\pi_x^2 1\pi_y^2 1\delta_+^2 1\delta_-^2\right\rangle$	1,254,468
$A^3\Delta$	5154/5196	0.957	1,075,778,714	4,884,866	0.928	0.893	$\left\|A\,^3\Delta\right\rangle_{A_1+A_2} \cong 0.89\left\|\frac{1}{\sqrt{2}}\left(1\sigma^2 2\sigma^2 3\sigma^1 1\pi_x^2 1\pi_y^2\right)\left(1\delta_+^1 1\delta_-^2 + 1\delta_+^2 1\delta_-^1\right)\right\rangle$	
$a^1\Delta$	3588/3392	0.956	587,898,192	3,356,266	0.926	0.890	$\left\|a\,^1\Delta\right\rangle_{A_1+A_2} \cong 0.89\left\|\frac{1}{\sqrt{2}}\left(1\sigma^2 2\sigma^2 3\bar{\sigma}^1 1\pi_x^2 1\pi_y^2\right)\left(1\delta_+^1 1\delta_-^2 + 1\delta_+^2 1\delta_-^1\right)\right\rangle$	
RhB								
$X^1\Sigma^+$	3588	0.959	587,898,192	3,356,266	0.938	0.903	$\left\|X\,^1\Sigma^+\right\rangle \cong 0.90\left\|1\sigma^2 2\sigma^2 1\pi_x^2 1\pi_y^2 1\delta_+^2 1\delta_-^2\right\rangle$	1,254,468
$A^3\Delta$	5154/5196	0.956	1,075,778,714	4,884,866	0.941	0.905	$\left\|a\,^3\Delta\right\rangle_{A_1+A_2} \cong 0.91\left\|\frac{1}{\sqrt{2}}\left(1\sigma^2 2\sigma^2 3\sigma^1 1\pi_x^2 1\pi_y^2\right)\left(1\delta_+^1 1\delta_-^2 + 1\delta_+^2 1\delta_-^1\right)\right\rangle$	
$a^1\Delta$	3588/3392	0.955	578,391,382	3,349,686	0.928	0.892	$\left\|A\,^1\Delta\right\rangle_{A_1+A_2} \cong 0.89\left\|\frac{1}{\sqrt{2}}\left(1\sigma^2 2\sigma^2 3\bar{\sigma}^1 1\pi_x^2 1\pi_y^2\right)\left(1\delta_+^1 1\delta_-^2 + 1\delta_+^2 1\delta_-^1\right)\right\rangle$	
PdBe								
$X^1\Sigma^+$	3588	0.960	587,898,192	3,356,266	0.949	0.915	$\left\|X\,^1\Sigma^+\right\rangle \cong 0.92\left\|1\sigma^2 2\sigma^2 1\pi_x^2 1\pi_y^2 1\delta_+^2 1\delta_-^2\right\rangle$	

$A^3\Sigma^+$	5196	0.959	1,089,179,112	6,091,522	0.961	0.927	$\left\|A\,^3\Sigma^+\right\rangle \cong 0.93\left\|1\sigma^2\,2\sigma^1\,3\sigma^1\,1\pi_x^2\,1\pi_y^2\,1\delta_+^2\,1\delta_-^2\right\rangle$	
$B^3\Delta$	5154/5196	0.959	1,075,778,714	4,884,866	0.975	0.935	$\left\|B^3\Delta\right\rangle_{A_1+A_2} \cong 0.94\left\|\frac{1}{\sqrt{2}}\left(1\sigma^2\,2\sigma^2\,3\sigma^1\,1\pi_x^2\,1\pi_y^2\right)\left(1\delta_+^1\,1\delta_-^2+1\delta_+^2\,1\delta_-^1\right)\right\rangle$	
$\alpha^1\Delta$	3588/3392	0.958	587,898,192	3,356,266	0.950	0.910	$\left\|a\,^1\Delta\right\rangle_{A_1+A_2} \cong 0.91\left\|\frac{1}{\sqrt{2}}\left(1\sigma^2\,2\sigma^2\,3\sigma^1\,1\pi_x^2\,1\pi_y^2\right)\left(1\delta_+^1\,1\delta_-^2+1\delta_+^2\,1\delta_-^1\right)\right\rangle$	

[a] MRCI Coefficient of reference C_0 CAS function.

Table S7. % Increase of bond lengths (R_e), dipole moment values calculated as expectation values ($<\mu>$) and by the finite field method (μ_{FF}), harmonic frequencies $\omega_{e,}$ dissociation energies (D_e^d, diabatic), (D_e^a, adiabatic) and (D_e^{gs}, with respect to ground state products) with respect to the corresponding TcN values of the corresponding states. The prime values are with respect to previous diatomic molecule, i.e., with respect to TcN for RuC, with respect to RuC and for RhB and with respect to RhB for PdBe.

		%													
State	**Methods**[a]	**R_e**	**R_e'**	**$<\mu>$**	**$<\mu>$'**	**μ_{FF}**	**μ_{FF}'**	**ω_e**	**ω_e'**	**D_e^d**	**D_e^{d}'**	**D_e^a**	**D_e^{a}'**	**D_e^{gs}**	**D_e^{gs}'**
RuC															
$X^1\Sigma^+$	MRCISD	0.8	0.8	-8.9	-8.9	-8.5	-8.5	-1.6	-1.6	9.0	9.0	10.1	10.1	51.0	51.0
	MRCISD+Q	0.7	0.7			-9.0	-9.0	-1.3	-1.3	10.2	10.2	9.7	9.7	50.3	50.3
	RCCSD(T)	0.6	0.6			-11.4	-11.4	-1.2	-1.2	15.4	15.4			59.2	59.2
$a^3\Delta$	MRCISD	2.1	2.1	-15.9	-15.9	-12.5	-12.5	-5.8	-5.8	14.9	14.9	14.9	14.9	26.7	26.7
	MRCISD+Q	2.1	2.1			-13.2	-13.2	-5.6	-5.6	16.6	16.6	16.6	16.6	28.9	28.9
$A^1\Delta$	MRCISD	2.2	2.2	5.3	5.3	0.2	0.2	-6.8	-6.8	14.2	14.2	14.2	14.2	33.9	33.9
	MRCISD+Q	2.2	2.2			-5.1	-5.1	-6.5	-6.5	14.5	14.5	14.5	14.5	35.8	35.8
RhB															
$X^1\Sigma^+$	MRCISD	5.2	6.0	-20.2	-27.3	-21.7	-28.4	-15.5	-16.9	-23.1	-16.1	-18.2	-9.9	-11.3	34.0
	MRCISD+Q	5.2	5.9			-23.1	-30.0	-15.4	-16.5	-23.4	-15.6	-18.4	-10.4	-13.5	30.0
	RCCSD(T)	5.5	6.2			-27.8	-36.1	-16.7	-17.7	-23.5	-11.7		-6.2	-15.7	34.3
$a^3\Delta$	MRCISD	8.2	10.5	-18.9	-31.8	-8.6	-20.0	-23.1	-27.6	-28.2	-17.5	-28.2	-17.5	-28.2	-9.0
	MRCISD+Q	8.2	10.5			-9.8	-21.7	-23.1	-27.4	-29.6	-17.9	-29.6	-17.9	-29.6	-9.3
$A^1\Delta$	MRCISD	8.7	11.0	45.7	53.4	-6.0	-5.8	-24.2	-29.3	-28.6	-18.5	-31.0	-21.2	-27.1	-2.4
	MRCISD+Q	8.5	10.9			-20.8	-24.8	-23.0	-28.1	-28.6	-18.3	-31.8	-21.9	-28.4	-2.8
PdBe															
$X^1\Sigma^+$	MRCISD	13.5	20.3	-50.3	-63.8	-62.5	-73.2	-32.4	-43.8	-63.9	-69.7	-63.9	-67.4	-61.3	-48.2
	MRCISD+Q	13.3	20.0			-68.1	-77.7	-32.2	-43.4	-60.9	-67.0	-60.9	-65.0	-58.2	-45.6
	RCCSD(T)	13.2	20.2			-72.6	-82.5	-32.5	-44.4	-63.2	-67.5	-63.2	-65.5	-60.7	-47.3
$b^3\Delta$	MRCISD	22.0	34.9	39.4	-4.9	-31.2	-45.0	-42.3	-58.2	-16.6	-31.3	-79.7	-83.3	-100.0	-100.0
	MRCISD+Q	21.4	34.2			-46.7	-58.2	-42.1	-58.0	-13.8	-29.3	-76.1	-80.4	-96.1	-96.4
$A^1\Delta$	MRCISD	21.4	34.8	24.5	90.9	18.8	11.9	-39.5	-57.2	-25.2	-39.0	-75.2	-80.4	-104.2	-104.1
	MRCISD+Q	21.1	34.3			-1.0	-25.6	-40.5	-57.2	-21.9	-36.1	-71.6	-77.9	-99.3	-99.3

Table S8. Energy (hartree), Bond length, R_e (Å), dissociation energy with respect to the ground state products D_e (kcal/mol), frequencies, ω_e (cm^{-1}), dipole moments μ(Debye) relative energy difference T_e (kcal/mol) of the M-X molecules

	State	Methodology	Energy	R_e	D_e	ω_e	μ	T_e
TcN	$^1\Sigma^+$	TPSSh/LANL2DZ	-134.625488	1.626	77.6	1176.1		23.7
		TPSSh/aug-cc-pVTZ$_X$(-PP)$_M$	-135.167273	1.581	96.5	1195.4		25.0
		TPSSh/aug-cc-pV5Z$_X$(-PP)$_M$	-135.173549	1.578	100.2	1196.0	4.493	25.1
	$^3\Delta$	TPSSh/LANL2DZ	-134.663194	1.644	101.3	1108.6		0.0
		TPSSh/aug-cc-pVTZ$_X$(-PP)$_M$	-135.207185	1.592	121.5	1156.5		0.0
		TPSSh/aug-cc-pV5Z$_X$(-PP)$_M$	-135.213594	1.589	125.3	1158.3	2.601	0.0
	$^5\Pi$	TPSSh/LANL2DZ	-134.640252	1.715	-86.9	946.4		14.4
		TPSSh/aug-cc-pVTZ$_X$(-PP)$_M$	-135.181461	1.567	105.4	985.5		16.1
RuC	$^1\Sigma^+$	TPSSh/LANL2DZ	-131.772668	1.644	119.0	1156.6		3.8
		TPSSh/aug-cc-pVTZ$_X$(-PP)$_M$	-132.533807	1.595	132.2	1176.4		6.2
		TPSSh/aug-cc-pV5Z$_X$(-PP)$_M$	-132.538025	1.592	132.5	1175.4	4.052	6.3
	$^3\Delta$	TPSSh/LANL2DZ	-131.778701	1.686	122.8	1048.4		0.0
		TPSSh/aug-cc-pVTZ$_X$(-PP)$_M$	-132.543742	1.628	138.4	1084.5		0.0
		TPSSh/aug-cc-pV5Z$_X$(-PP)$_M$	-132.548064	1.625	138.8	1084.1	2.247	0.0
	$^5\Pi$	TPSSh/LANL2DZ	-131.708681	1.781	-78.8	850.0		43.9
		TPSSh/aug-cc-pVTZ$_X$(-PP)$_M$	-132.473100	1.715	94.1	890.2		44.3
RhB	$^1\Sigma^+$	TPSSh/LANL2DZ	-134.190952	1.747	107.7	935.2		0.0
		TPSSh/aug-cc-pVTZ$_X$(-PP)$_M$	-134.939635	1.689	121.0	958.9		0.0
		TPSSh/aug-cc-pV5Z$_X$(-PP)$_M$	-134.942636	1.684	121.2	958.0	3.0078	0.0
	$^3\Delta$	TPSSh/LANL2DZ	-134.166627	1.838	92.5	793.5		15.3
		TPSSh/aug-cc-pVTZ$_X$(-PP)$_M$	-134.916538	1.773	106.5	813.2		14.5
		TPSSh/aug-cc-pV5Z$_X$(-PP)$_M$	-134.919484	1.769	106.7	812.5	1.862	14.5
	$^5\Pi$	TPSSh/LANL2DZ	-134.085282	2.000	-41.4	562.7		66.3
		TPSSh/aug-cc-pVTZ$_X$(-PP)$_M$	-134.831866	1.939	53.3	589.7		67.6
PdBe	$^1\Sigma^+$	TPSSh/LANL2DZ	-141.365215	1.977	54.1	635.7		0.0
		TPSSh/aug-cc-pVTZ$_X$(-PP)$_M$	-142.153312	1.916	58.1	647.0		0.0
		TPSSh/aug-cc-pV5Z$_X$(-PP)$_M$	-142.155127	1.909	58.6	649.0	0.750	0.0
	$^3\Sigma^+$	TPSSh/LANL2DZ	-141.317860	2.111	24.4	518.1		29.7
		TPSSh/aug-cc-pVTZ$_X$(-PP)$_M$	-142.107019	2.060	29.1	516.1		29.0
		TPSSh/aug-cc-pV5Z$_X$(-PP)$_M$	-142.108636	2.054	29.5	515.0	0.628	29.2
	$^5\Pi$	TPSSh/LANL2DZ	-141.190731	2.271	-55.4	376.9		109.5
		TPSSh/aug-cc-pVTZ$_X$(-PP)$_M$	-141.986474	2.192	-46.6	430.3		104.7

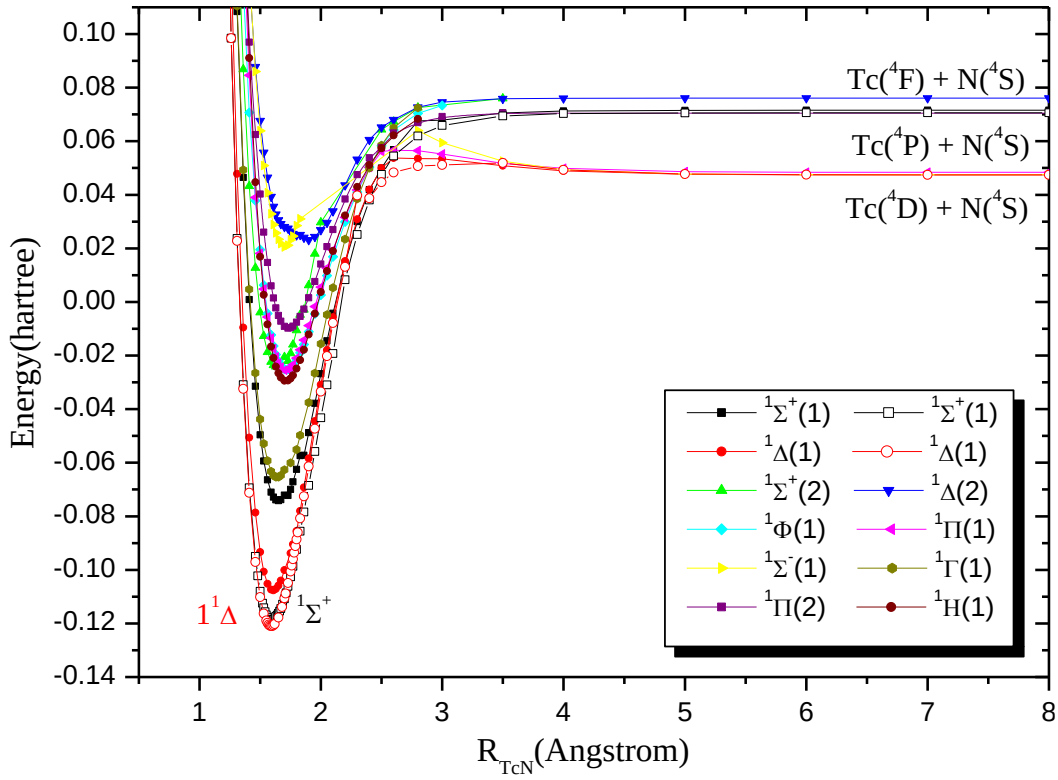

Figure S1. CASSCF(12,10)/aug-cc-pV5Z$_N$(-PP)$_{Tc}$ potential energy curves of ten singlet states of the TcN molecule. Solid points correspond to SA-CASSCF, hollow points corresponds to CASSCF (single root). Zero energy corresponds to the atomic ground states products.

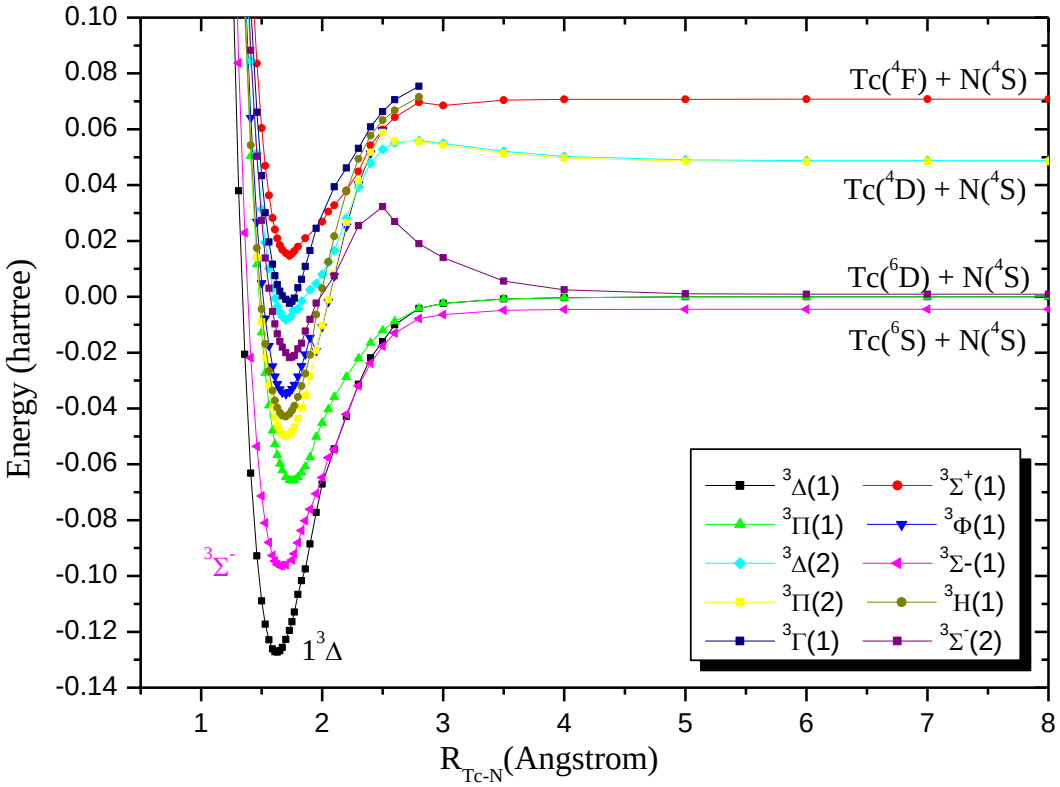

Figure S2. CASSCF(12,10)/aug-cc-pV5Z$_N$(-PP)$_{Tc}$ potential energy curves of ten triplet states of the TcN molecule. Zero energy corresponds to the atomic ground states products.

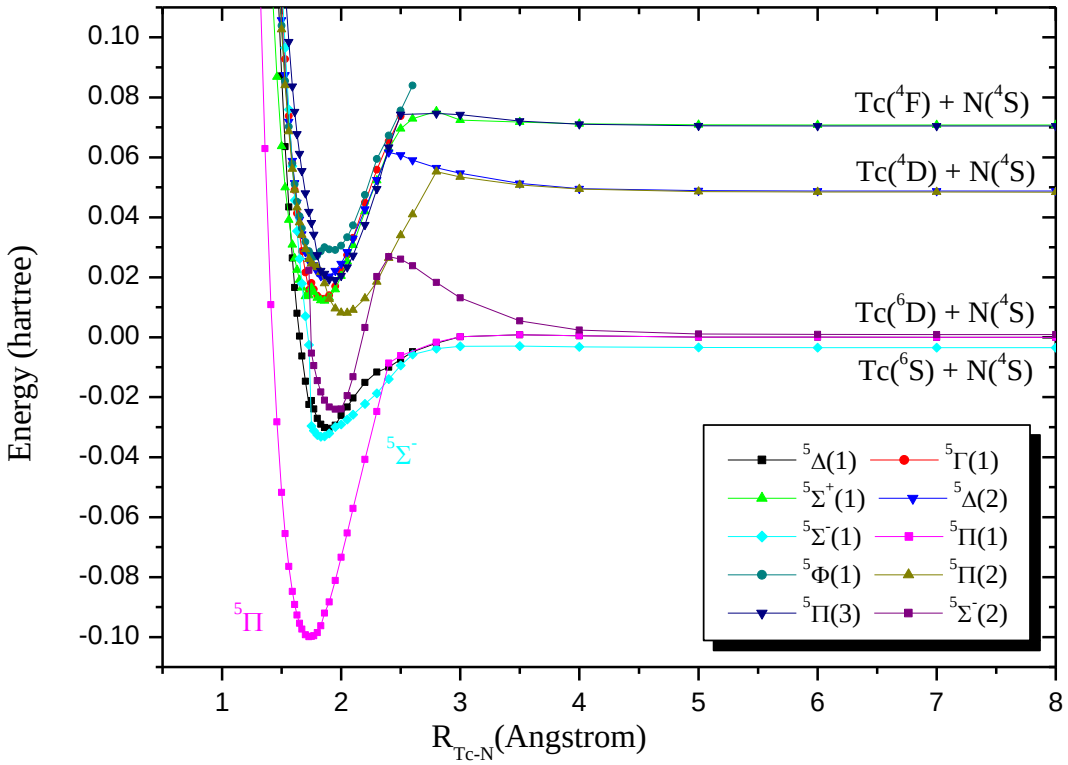

Figure S3. CASSCF(12,10)/aug-cc-pV5Z$_N$(-PP)$_{Tc}$ potential energy curves of ten quintet states of the TcN molecule. Zero energy corresponds to the atomic ground states products.

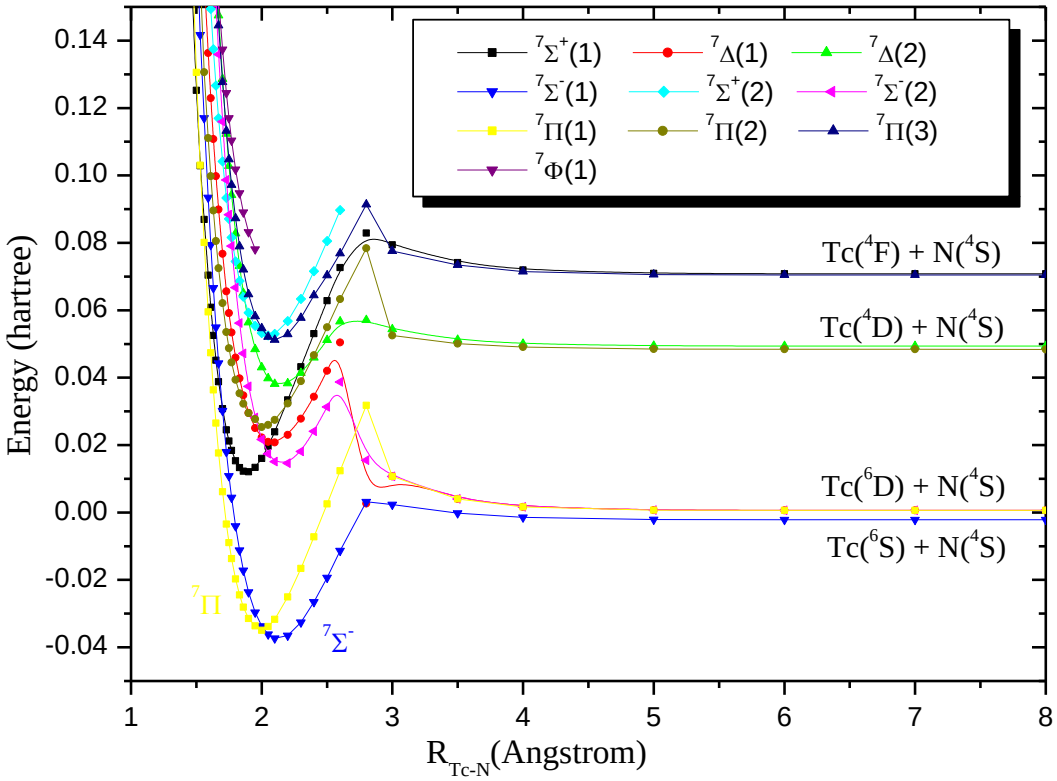

Figure S4. CASSCF(12,10)/aug-cc-pV5Z$_N$(-PP)$_{Tc}$ potential energy curves of ten septet states of the TcN molecule. Zero energy corresponds to the atomic ground states products.

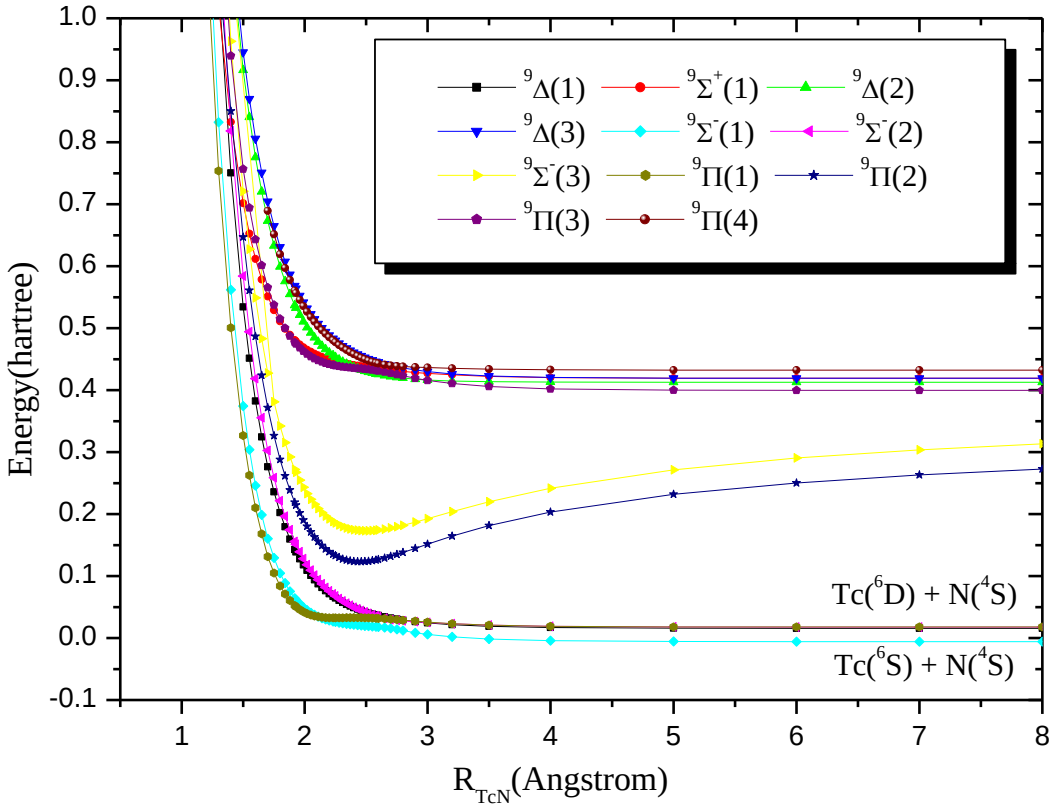

Figure S5. CASSCF(12,10)/aug-cc-pV5Z$_N$(-PP)$_{Tc}$ potential energy curves of eleven nonet states of the TcN molecule. Zero energy corresponds to the atomic ground states products.

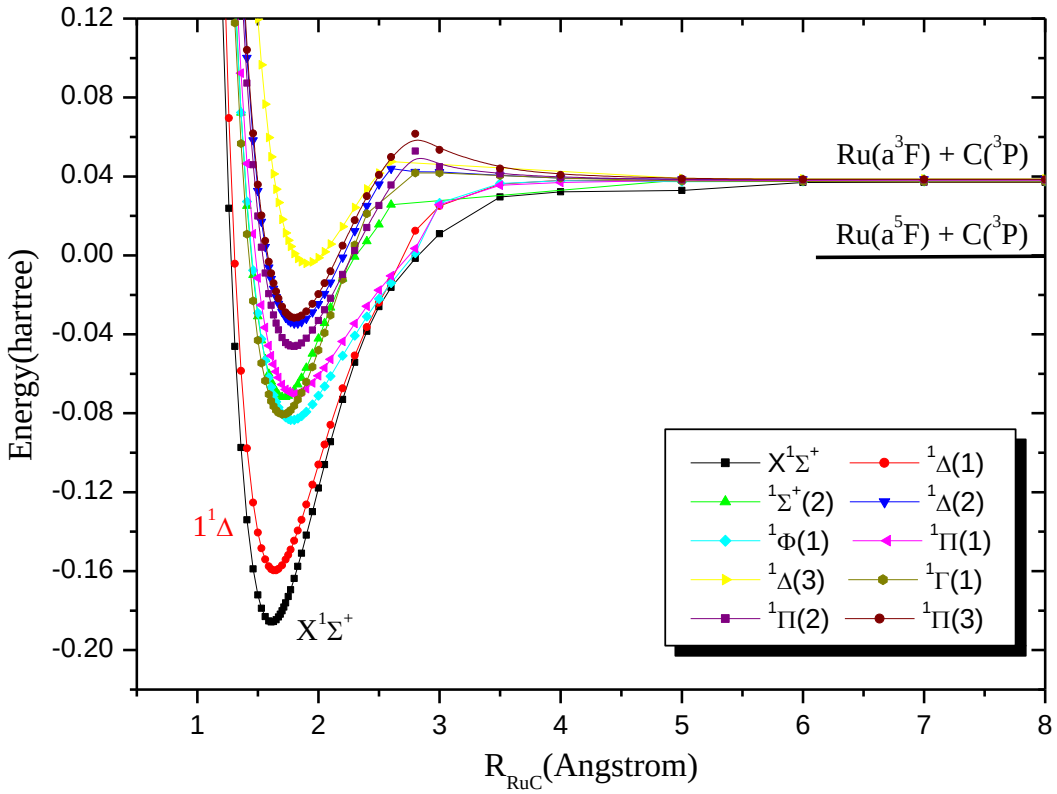

Figure S6. CASSCF(12,10)/aug-cc-pV5Z$_C$(-PP)$_{Ru}$ potential energy curves of ten singlet states of the RuC molecule. Zero energy corresponds to the atomic ground states products.

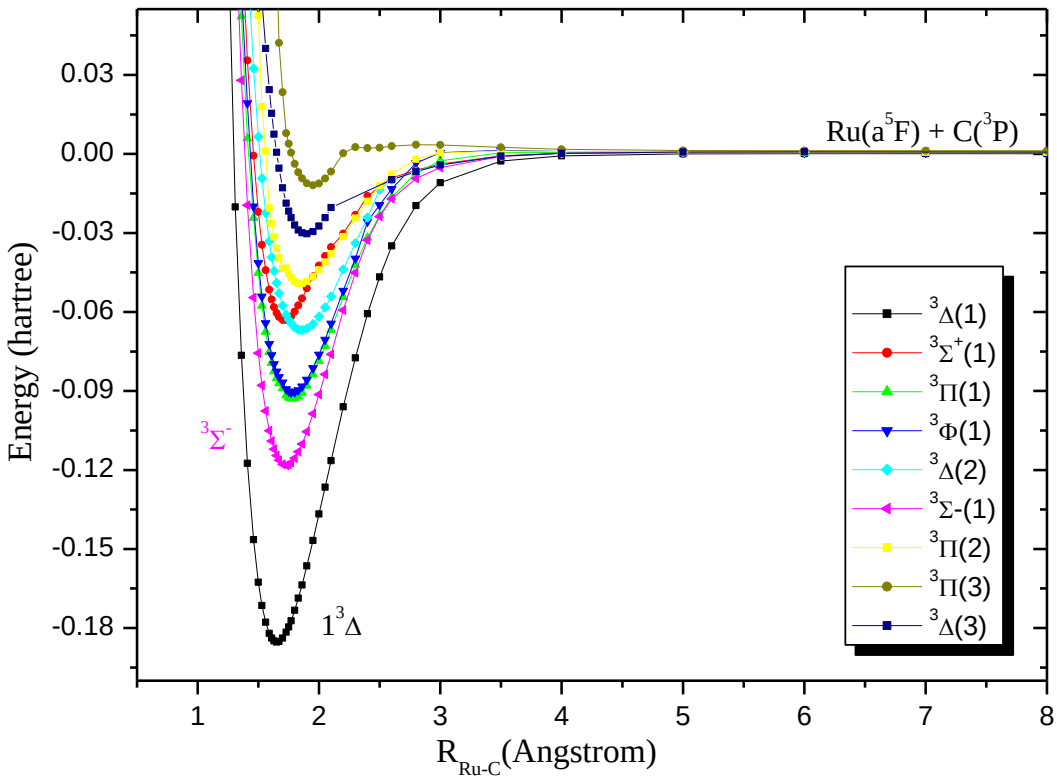

Figure S7. CASSCF(12,10)/aug-cc-pV5Z$_C$(-PP)$_{Ru}$ potential energy curves of nine triplet states of the RuC molecule. Zero energy corresponds to the atomic ground states products.

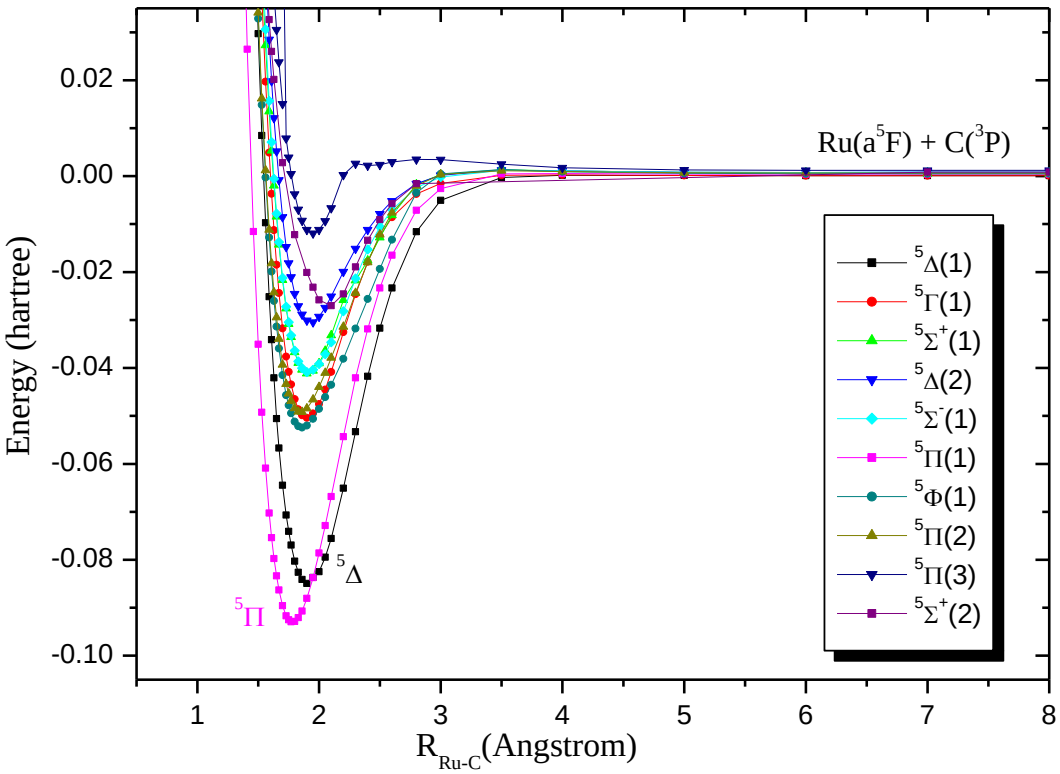

Figure S8. CASSCF(12,10)/aug-cc-pV5Z$_C$(-PP)$_{Ru}$ potential energy curves of ten quintet states of the RuC molecule. Zero energy corresponds to the atomic ground states products.

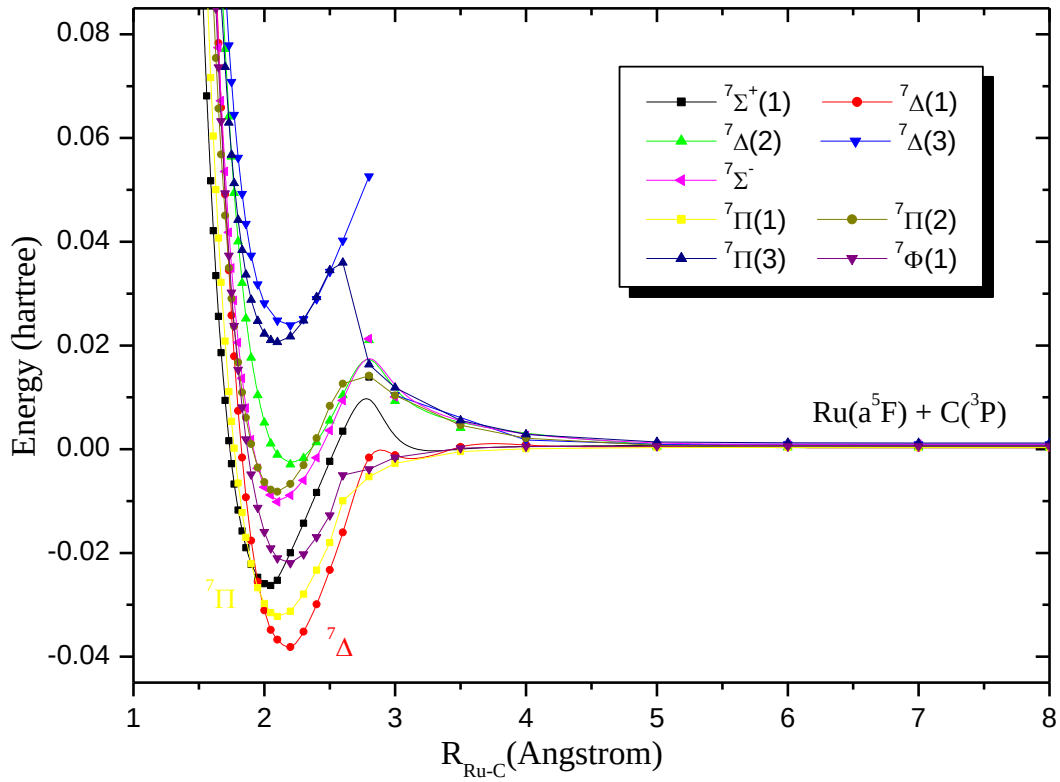

Figure S9. CASSCF(12,10)/aug-cc-pV5Z$_C$(-PP)$_{Ru}$ potential energy curves of nine septet states of the RuC molecule. Zero energy corresponds to the atomic ground states products.

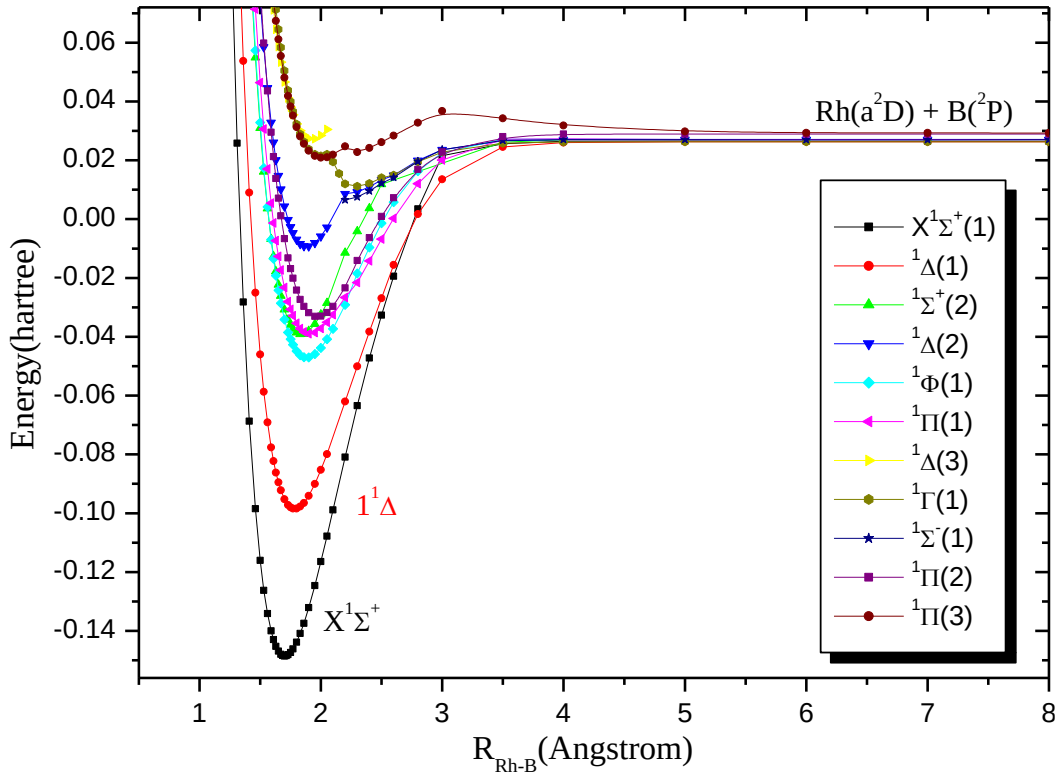

Figure S10. CASSCF(12,10)/aug-cc-pV5Z$_{B}$(-PP)$_{Rh}$ potential energy curves of eleven singlet states of the RhB molecule. Zero energy corresponds to the atomic ground states products.

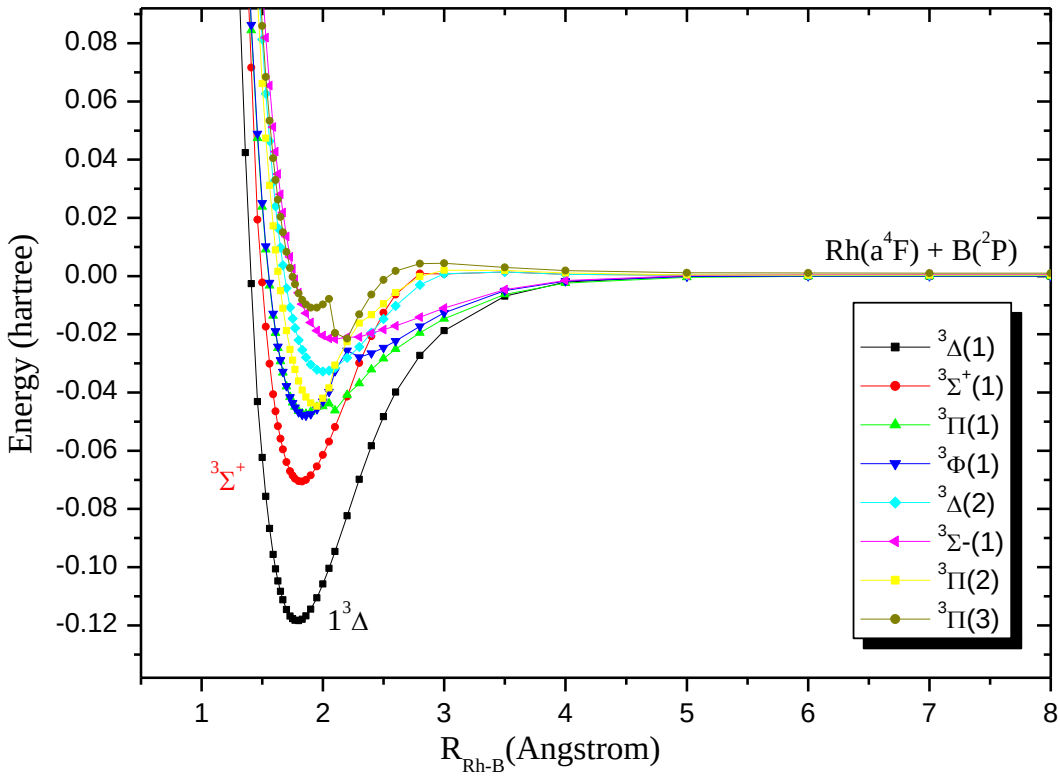

Figure S11. CASSCF(12,10)/aug-cc-pV5Z$_{B}$(-PP)$_{Rh}$ potential energy curves of eight triplet states of the RhB molecule. Zero energy corresponds to the atomic ground states products.

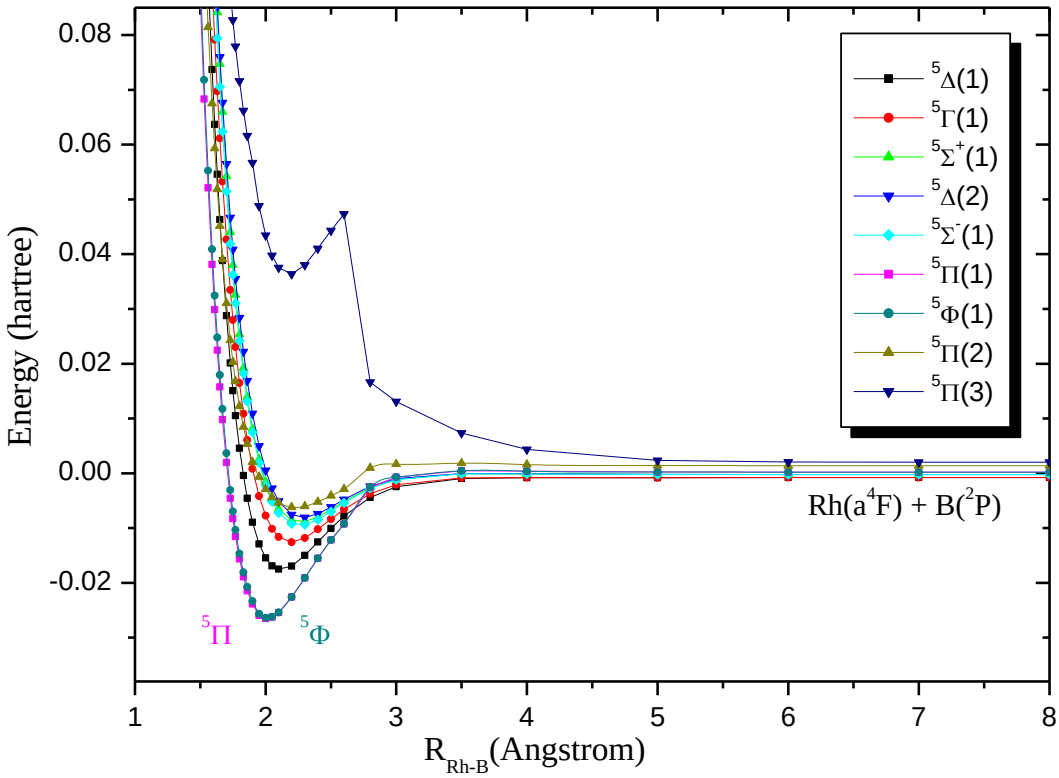

Figure S12. CASSCF(12,10)/aug-cc-pV5Z$_{B}$(-PP)$_{Rh}$ potential energy curves of nine quintet states of the RhB molecule. Zero energy corresponds to the atomic ground states products.

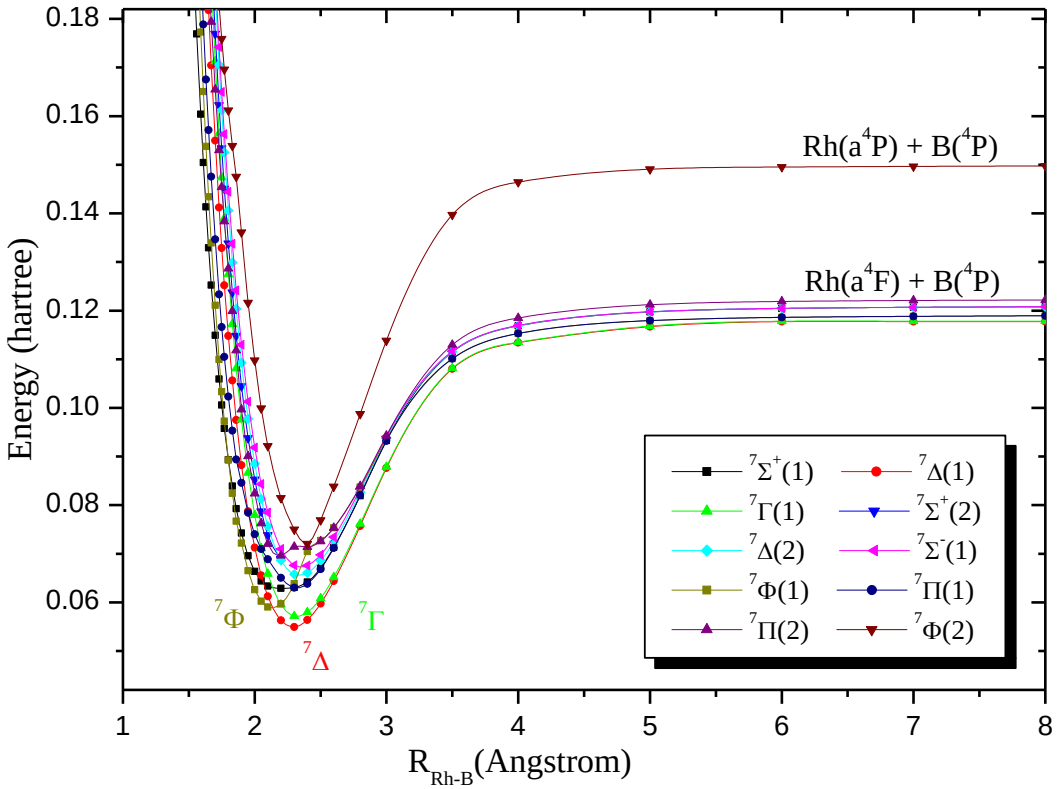

Figure S13. CASSCF(12,10)/aug-cc-pV5Z$_{B}$(-PP)$_{Rh}$ potential energy curves of ten septet states of the RhB molecule. Zero energy corresponds to the atomic ground states products.

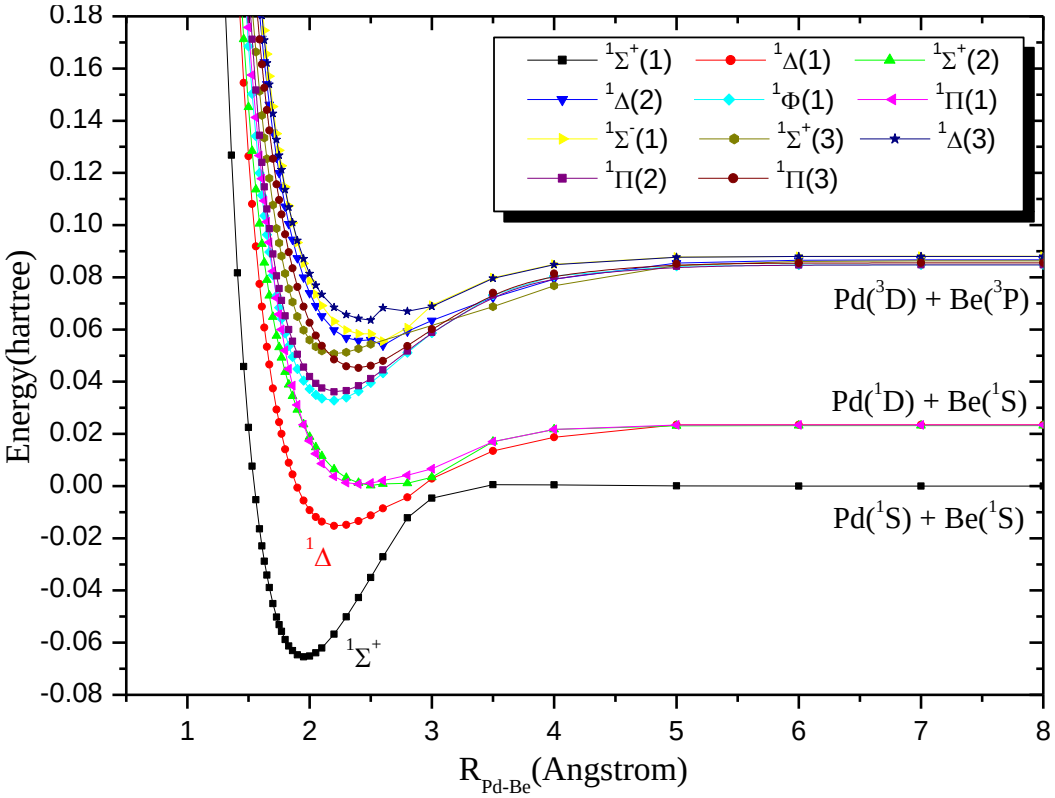

Figure S14. CASSCF(12,10)/aug-cc-pV5Z$_{B}$(-PP)$_{Pd}$ potential energy curves of eleven singlet states of the PdBe molecule. Zero energy corresponds to the atomic ground states products.

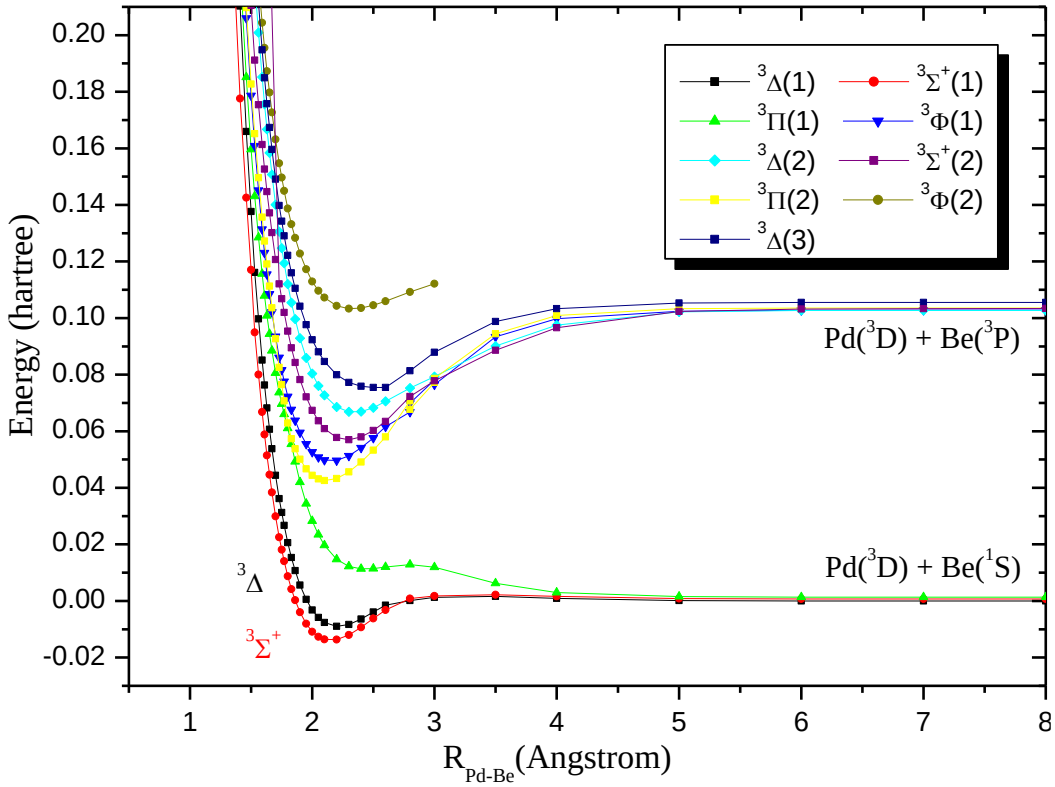

Figure S15. CASSCF(12,10)/aug-cc-pV5Z$_{Be}$(-PP)$_{Pd}$ potential energy curves of nine triplet states of the PdBe molecule. Zero energy corresponds to the lowest involved atomic states products.

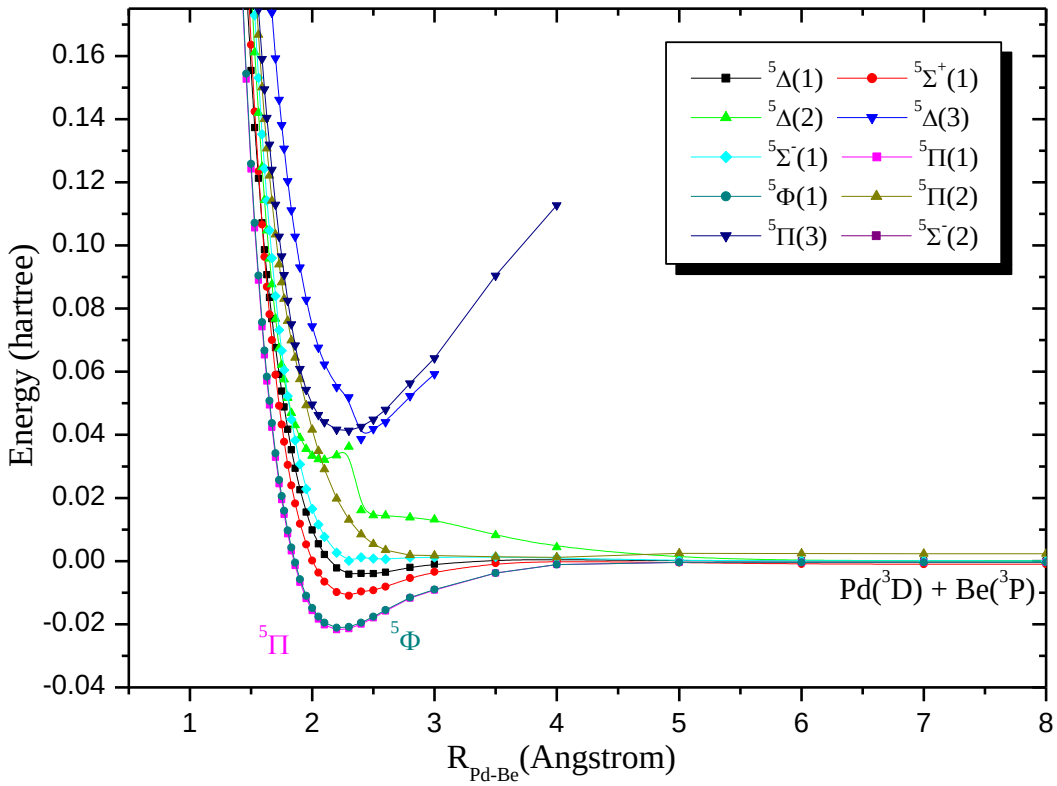

Figure S16. CASSCF(12,10)/aug-cc-pV5Z$_{Be}$(-PP)$_{Pd}$ potential energy curves of ten quintet states of the PdBe molecule. Zero energy corresponds to the lowest involved atomic states products.

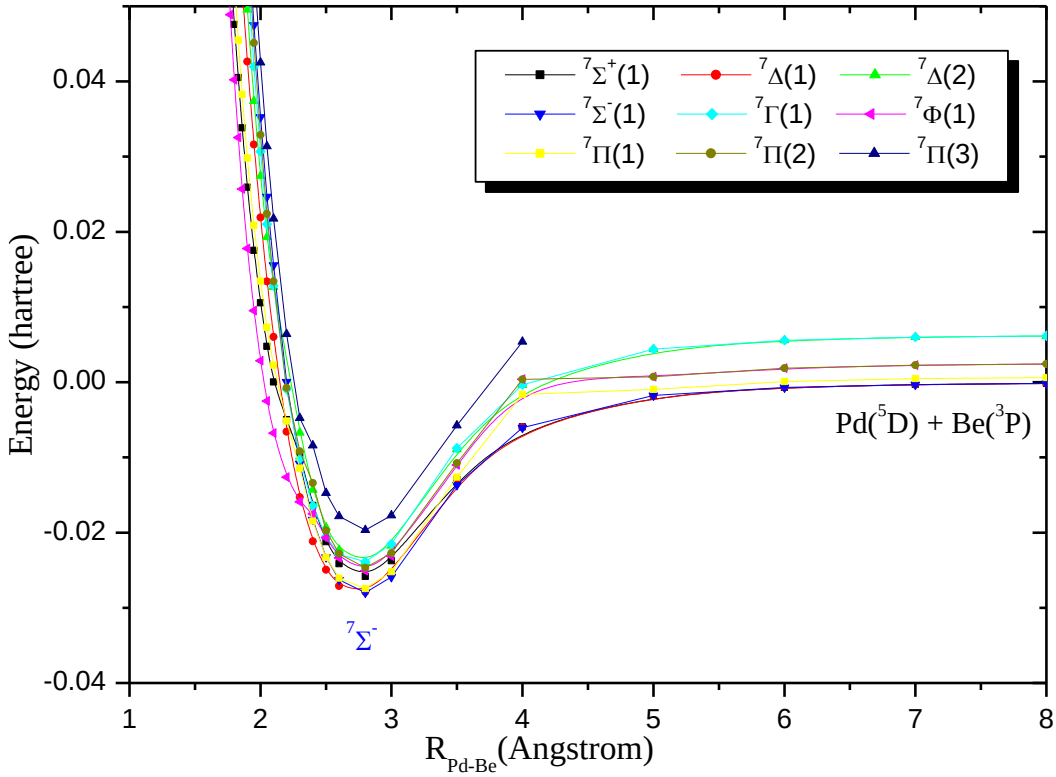

Figure S17. CASSCF(12,10)/aug-cc-pV5Z$_{Be}$(-PP)$_{Pd}$ potential energy curves of ten septet states of the PdBe molecule. Zero energy corresponds to the lowest involved atomic states products.

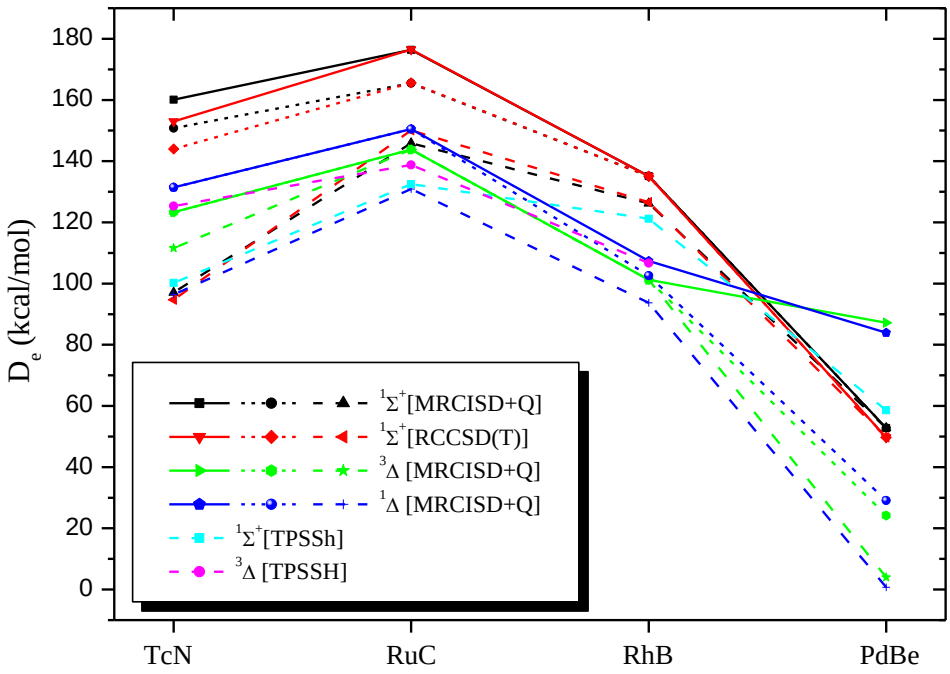

Table S18. Dissociation energies D_e (diabatic, D_e^d: solid line, adiabatic, D_e^a: dot line, with respect to the atomic ground state, D_e^{gs}: dash line) of the $^1\Sigma^+$, $^3\Delta$, and $^1\Delta$ states of the M-X molecules at different levels of theory using the aug-cc-pV5Z$_X$(-PP)$_M$ basis set.

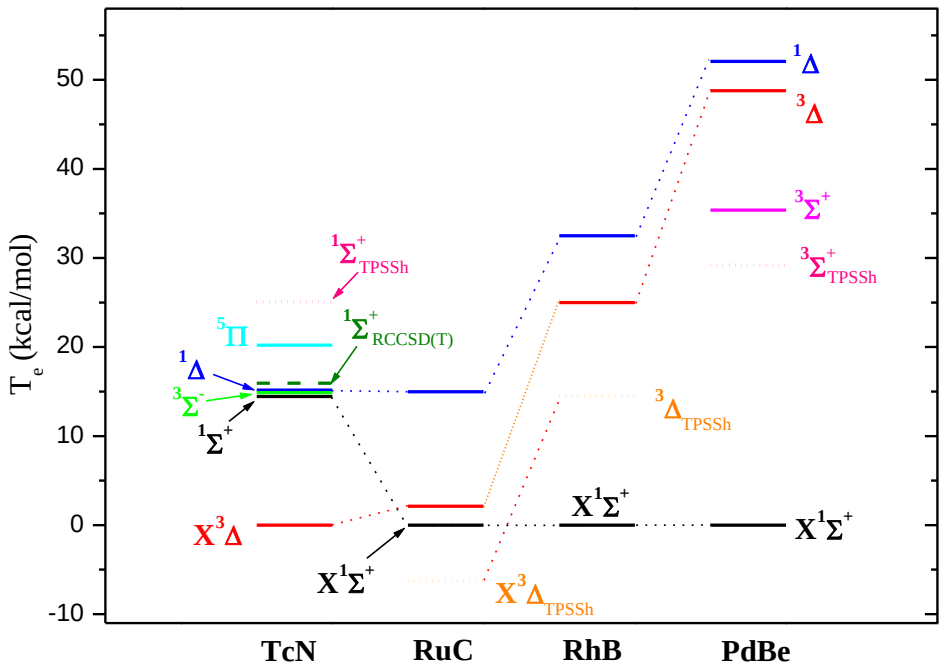

Figure S19. Relative energy levels (T_e) of the lowest in energy states of the MX molecules with respect to the ground states of MX at the MRCISD+Q(solid lines), RCCSD(T)(dash lines), and TPSSh(dot lines) /aug-cc-pV5Z$_X$(–PP)$_M$ levels of theory.

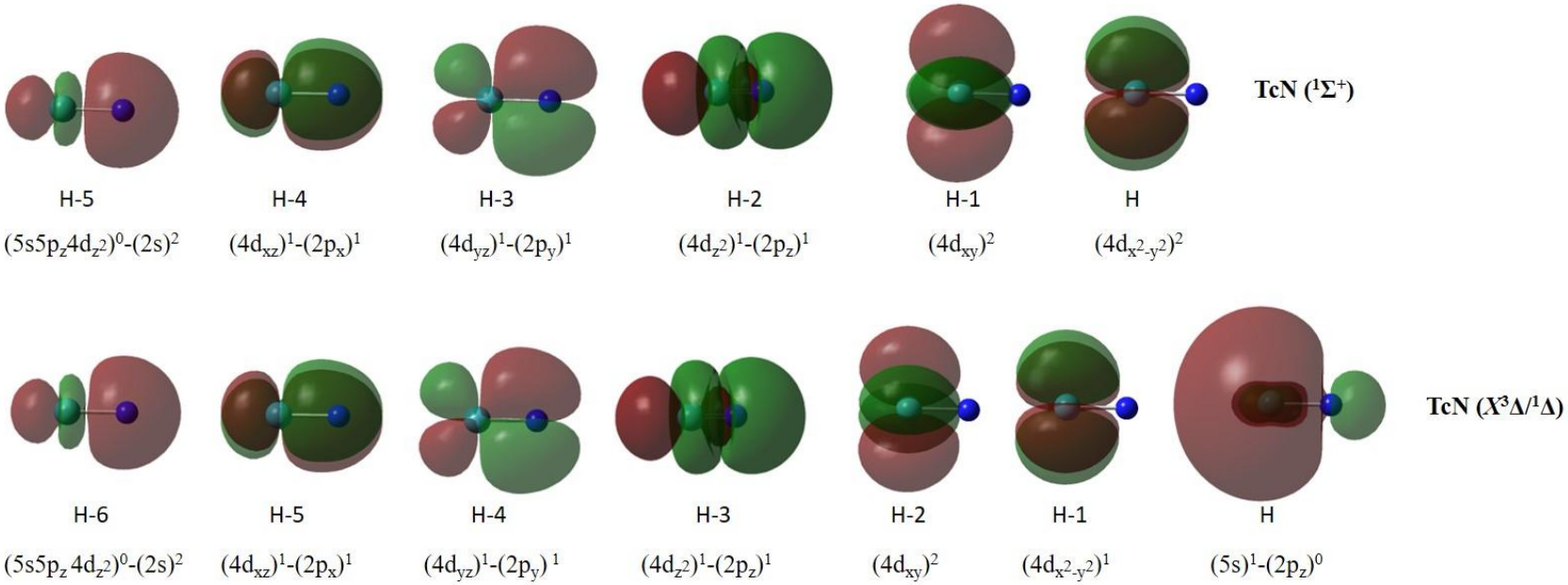

Figure S20. Molecular Orbitals of the $X^3\Delta$, $^1\Sigma^+$, and $^1\Delta$ states of the TcN molecule. The main atomic orbitals involved in MO are reported.

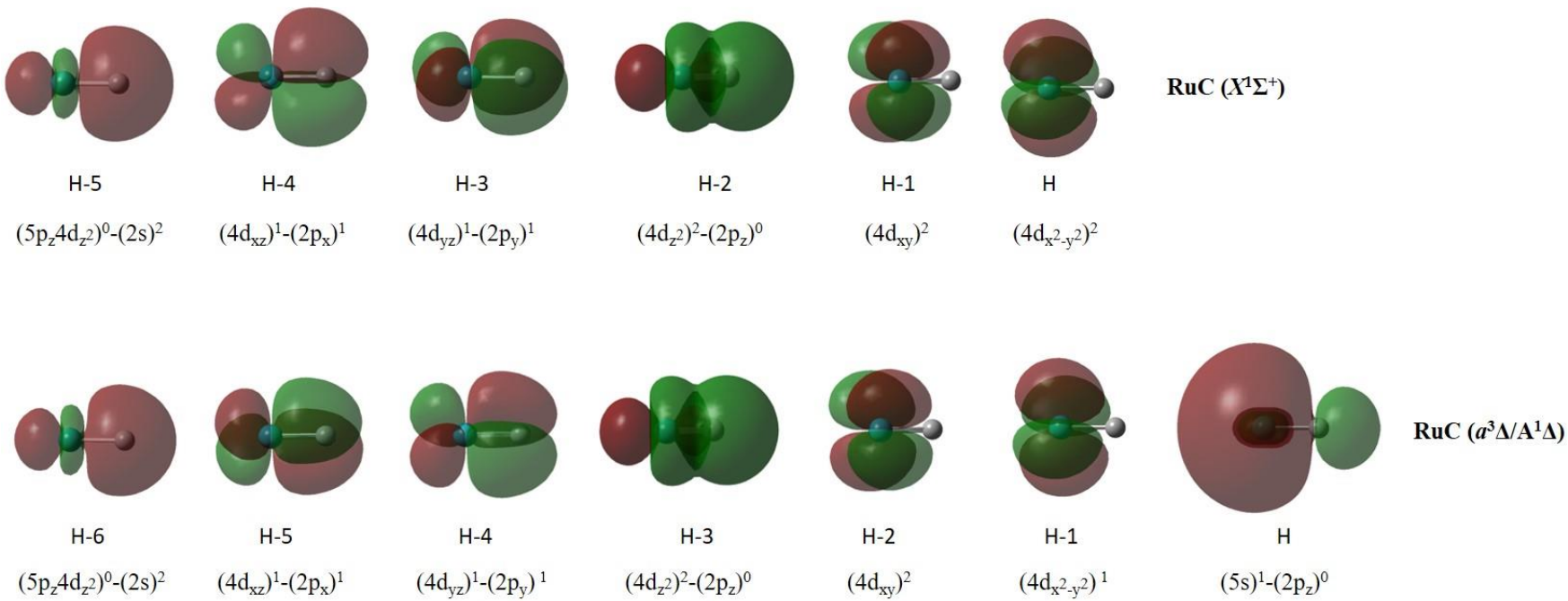

Figure S21. Molecular Orbitals of the $X^1\Sigma^+$ $a^3\Delta$, and $A^1\Delta$ states of the RuC molecule. The main atomic orbitals involved in MO are reported.

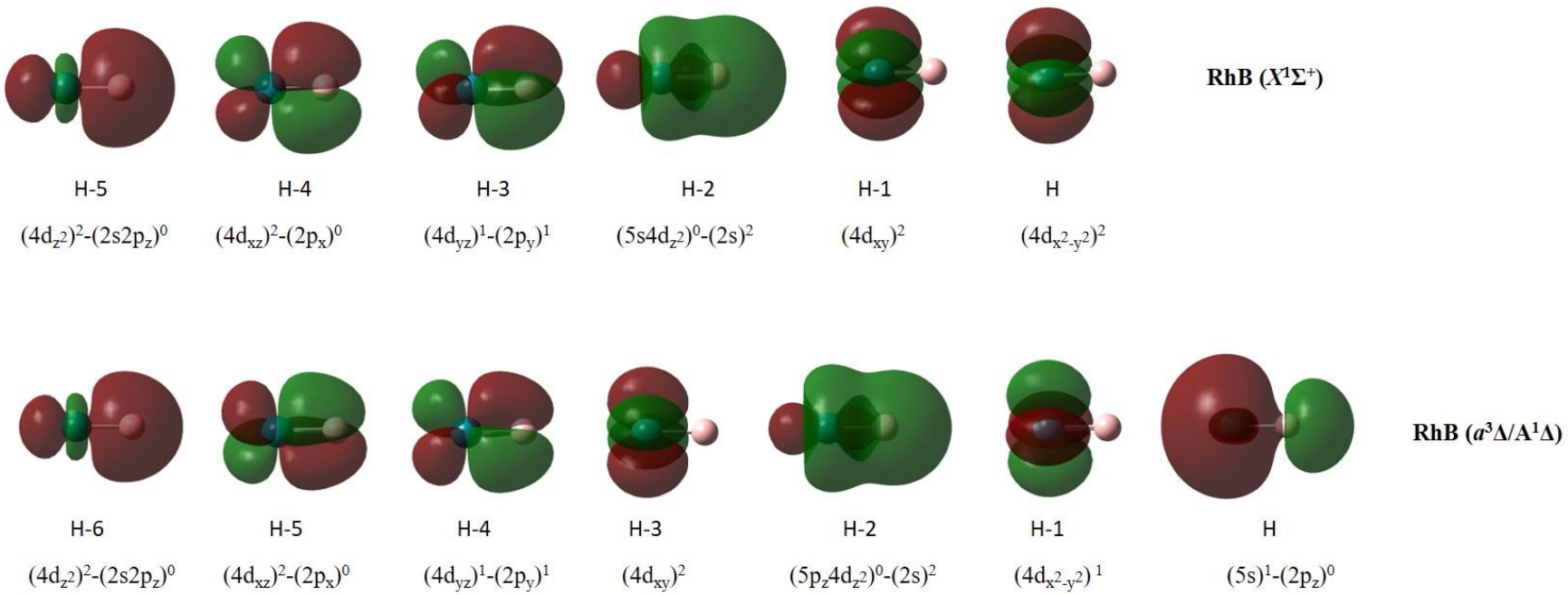

Figure S22. Molecular Orbitals of the $X^1\Sigma^+$, $a^3\Delta$, and $A^1\Delta$ states of the RhB molecule. The main atomic orbitals involved in MO are reported.

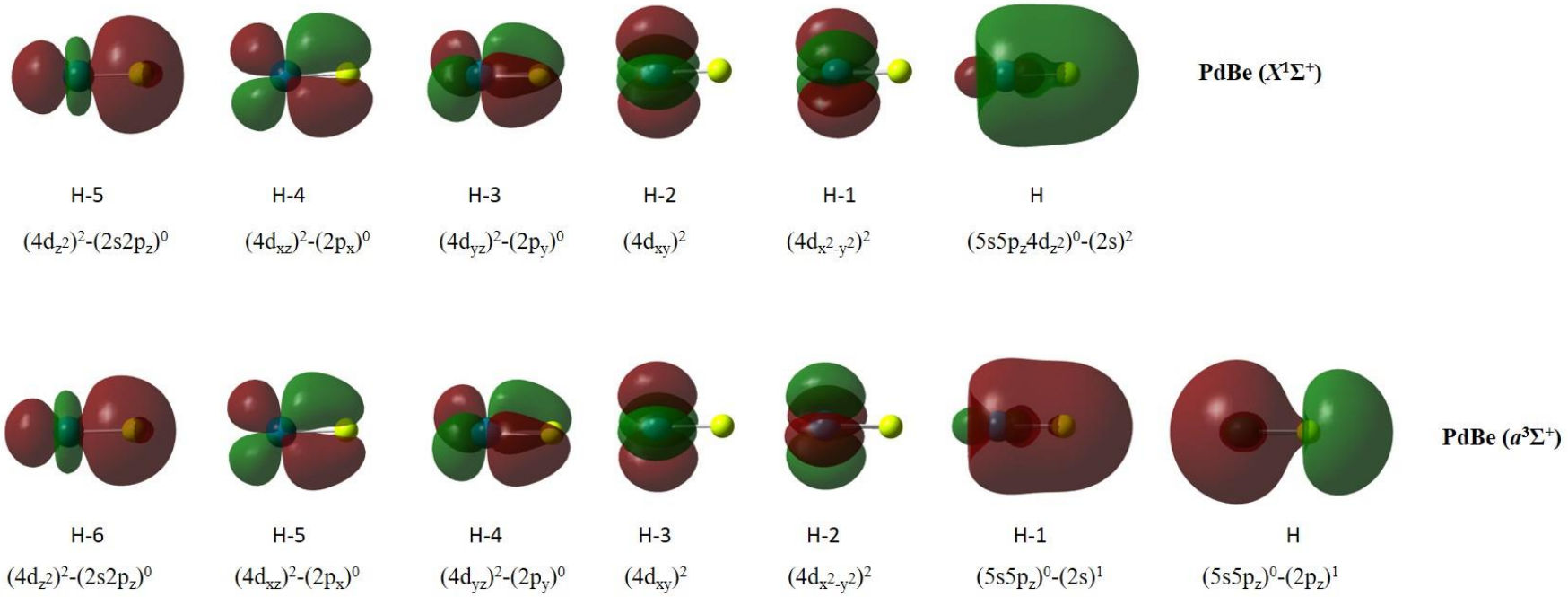

Figure S23. Molecular Orbitals of the $X^1\Sigma^+$ and $a^3\Sigma^+$ states of the PdBe molecule. The main atomic orbitals involved in MO are reported.